Cellular Physiology and Biochemistry

Cell Physiol Biochem 2013;31:703-717
DOI: 10.1159/000350089
Published online: May 16, 2013
Accepted: April 22, 2013

1421-9778/13/0315-0703$38.00/0

Original Paper

Sox9 Modulates Proliferation and Expression of Osteogenic Markers of Adipose-Derived Stem Cells (ASC)

Sabine Stöckl[a,b] Claudia Göttl[a,b] Joachim Grifka[b] Susanne Grässel[a,b]

[a]Centre for Medical Biotechnology, BioPark I, University of Regensburg, Regensburg, Germany;
[b]Orthopaedic Surgery, Experimental Orthopaedics, University of Regensburg, Regensburg, Germany

Key Words
Sox9 • Osteocalcin • Adipose-derived stem cell • Proliferation • Osteogenesis

Abstract
Background: Mesenchymal stem cells (MSC) are promising tools for tissue-engineering and musculoskeletal regeneration. They reside within various tissues, like adipose tissue, periosteum, synovia, muscle, dermis, blood and bone marrow, latter being the most common tissue used for MSC isolation. A promising alternative source for MSC is adipose tissue due to better availability and higher yield of MSC in comparison to bone marrow. A drawback is the yet fragmentary knowledge of adipose-derived stem cell (ASC) physiology in order to make them a safe tool for *in vivo* application. ***Methods/Results:*** Here, we identified Sox9 as a highly expressed and crucial transcription factor in undifferentiated rat ASC (rASC). In comparison to rat bone marrow-derived stem cells (rBMSC), mRNA and protein levels of Sox9 were significantly higher in rASC. To study the role of Sox9 in detail, we silenced Sox9 with shRNA in rASC and examined proliferation, apoptosis and the expression of osteogenic differentiation markers. Our results clearly point to a difference in the expression profile of osteogenic marker genes between undifferentiated rASC and rBMSC in early passages. Sox9 silencing induced the expression of *osteocalcin, Vegfα* and *Mmp13*, and decreased rASC proliferation accompanied with an induction of p21 and cyclin D1 expression and delayed S-phase entry. ***Conclusions:*** We suggest a pro-proliferative role for Sox9 in undifferentiated rASC which may explain the higher proliferation rate of rASC compared to rBMSC. Moreover, we propose an osteogenic differentiation delaying role of Sox9 in rASC which suggests that Sox9 expression is needed to maintain rASC in an undifferentiated, proliferative state.

Susanne Grässel, Ph.D.

Dept. of Orthopaedics, University of Regensburg
ZMB / BioPark 1, Josef-Engert-Str. 9, 93053 Regensburg (Germany)
Tel.+49 941-943-5065, Fax+49-941-943-5066
E-Mail susanne.graessel@klinik.uni-regensburg.de

Introduction

Mesenchymal stem cells (MSC) are able to self-renew and to differentiate into several lineages, i.e. chondrocytes, osteocytes or adipocytes and thus MSC are a highly attractive alternative for usage in tissue-engineering and regenerative medicine.

In the past, adult MSC were commonly isolated from bone marrow. Bone marrow-derived stem cells (BMSC) form only 0.001– 0.01% of total nucleated cells in the aspirate [1] and, require therefore a considerable amount of primary cell material or a time consuming expansion period. Moreover, comorbidity constitutes a problem, as it is always required to induce a bone defect to aspirate the bone marrow.

Today it is known that MSC can be found in nearly all adult tissues, e.g. adipose tissue, dermis, periosteum, peripheral and menstrual blood and in solid organs like liver, spleen and lung [2-4]. Therefore, adipose-derived MSC (ASC) qualify as an excellent alternative to BMSC. Advantages are the abundance of adipose tissue in the body of mammals and its easy accessibility as it is often prone to disposal as medical waste [5]. In addition, the method of obtaining a lipo-aspirate is less invasive and expensive which is in part attributable to the fact that adipose tissue displays a 2500-fold higher frequency of stem cells compared to bone marrow [6]. Molecular characteristics in terms of their immunosuppressive properties show that ASC behave similar to BMSC [7]. Recent studies related to bone tissue-engineering using ASC in combination with several clinically available biomaterials and scaffolds show promising results.

In a self-designed bioreactor, Fröhlich et al. cultured a scaffold construct seeded with human ASC and reported a profound increase in osteogenic differentiated cells and bone matrix formation [8]. Animal model studies support the idea that ASC are of interest for the fabrication of tissue-engineered bone *in vitro.* Notable, autologous ASC improved bone regeneration in a critical-sized skull defect of adult New Zealand white rabbits, when they were implanted after pre-osteogenic induction together with a fibronectin-coated porous cylindrical PLA (poly-L-lactic acid) scaffold [9].

It is known that culture time and passage number of MSC in general, and ASC in particular crucially affect their biological activities and their immunophenotype.

Different studies have compared and characterized the immunophenotype of freshly isolated ASC with serial passaged ASC, and found that during culture time the expression profile of stromal cell associated surface markers and colony forming unit capacity changed progressively while other markers as endothelial associated molecules remained unaffected [10, 11]. One reason is certainly the well known heterogeneity of fresh ASC preparations which most likely affects biological properties beside the expression of surface markers. Further, it is described that long-term *in vitro* expansion of human ASC affects osteogenic differentiation capacity negatively and increases cell senescence. After long-term *in vitro* expansion culture, ASC were able to differentiate into immature osteoblast-like cells only [12, 13]. Hence, a short-term expansion period of undifferentiated ASC in combination with the requirement to receive a sufficient number of cells is highly desirable for optimal therapeutically use. In this light, the physiology of ASC needs still in depth characterization to assure that there is no loss or alteration of the cellular or molecular phenotype during *ex vivo* culture and differentiation and subsequent *in vivo* application.

Sox9 is mainly described as the master transcription factor for chondrogenic differentiation and is expressed in all osteo-chondroprogenitor cells and chondrocytes. It is required for mesenchymal condensation and inhibition of precocious hypertrophic conversion of proliferating chondrocytes during embryonic chondrogenesis [14, 15]**.** Several recent studies have demonstrated that Sox9 is also well expressed in adult tissues [16]. Sox9 is not only crucial for chondrogenic differentiation of BMSC [17, 18] but also of MSC from other sources. Yang et al. showed that Sox9 facilitates the differentiation of adipose tissue-derived stem cells into a chondrocyte-like phenotype *in vitro* [19].

In addition to its critical involvement in chondrogenic differentiation during musculoskeletal development, Akiyama et al. suggest that osteo-chondroprogenitor

cells, derived from mesenchymal stem cells, adopt an osteogenic phenotype when Sox9 expression is lower than Runx2 expression which is supported by a delayed endochondral bone formation in Sox9 knock-in heterozygous mutant mice [16, 20]. In addition, when Sox9 is ectopically overexpressed in Runx2-expressing osteoblasts, the following ossification process appears abnormal, indicating that Sox9 is able to inhibit regulators of osteoblast development [21]. The role of Sox9 for chondrogenesis has already been thoroughly studied in BMSC [17, 22, 23] as well as in ASC [24] but only little is known about the role of Sox9 in undifferentiated MSC and BMSC or ASC osteogenesis [25]. Lee et al. determined in their study the potential of SOX-trio co-transduced ASC (Sox9, Sox5 and Sox6) to repair osteochondral defects and to delay the progression of osteoarthritic lesions in a rat model and showed thereby a strong evidence for a beneficial effect of Sox9 on osteochondral defect healing in a surgically-induced osteoarthritis model [24]. Besides being an important transcription factor for proper differentiation and developmental processes, Sox9 is moreover known to affect the proliferation and cell cycle distribution in several cells and tissues. In lung adenocarcinoma, a Sox9 knockdown resulted in an upregulation of p21 and thus in a marked decrease of adhesive and anchorage-independent growth and is suggested to contribute to gain of tumor growth potential, possibly acting through affecting the expression of cell cycle regulators p21 and CDK4 [26]. P21 is well known as an negative regulator of the cell cycle [27], but recently other roles for p21 beside being a cell cycle inhibitor are reported. In this context, apoptosis, hypertrophy and cell morphology in different cell types could be affected via p21, depending on the subcellular localization of the protein [28].

In this study, we detected a strong induction of Sox9 in ASC compared to BMSC, and in addition differences in gene expression profile related to osteogenic differentiation. We therefore focused on Sox9 and observed an impact of this transcription factor on proliferation of ASC, accompanied by an increased p21 and cyclin D1 protein expression. Silencing Sox9 had a clearly stimulating effect on *osteocalcin* and *Mmp13* gene expression in undifferentiated and osteogenic differentiated ASC. Matrix mineralization as an indicator for successful osteogenic differentiation is also reduced after Sox9 silencing.

Materials and Methods

Isolation and culture of rASC and rBMSC

MSC were isolated from the subcutaneous adipose tissue [29, 30] and bone marrow [31] of five week old CD-rats and cultured in monolayer in appropriate media until reaching ~ 80% confluence. Until the first detachment from the cell culture flask using Trypsin-EDTA (Sigma, St.Louis, Missouri, USA), cells are defined as passage 0.

Bone marrow-derived MSC (rBMSC) were cultured in α-MEM (Life Technologies, Carlsbad, California, USA), supplemented with 10% fetal calf serum (FCS), 1% Penicillin-Streptomycin (P/S) (all Sigma, St.Louis, Missouri, USA) and 2% GLUTAMAX (Life Technologies, Carlsbad, California, USA), and adipose-derived MSC (rASC) in DMEM-F12 with 10% FCS and 1% P/S (all Sigma, St.Louis, Missouri, USA).

Flow cytometry

Immunophenotyping. After blocking with 5% mouse serum (Millipore, Billerica, Massachusetts, USA), passage 1 and passage 2 cells ($1x10^6$) were suspended in PBS containing following conjugated antibodies each: FITC-coupled antibody against CD90 (Becton Dickinson, Franklin Lakes, New Jersey, USA, #554897), PE-coupled antibody against CD11b (Becton Dickinson, Franklin Lakes, New Jersey, USA, # 562105), PE-Cy5-coupled antibody against CD45 (Becton Dickinson, Franklin Lakes, New Jersey, USA, # 559135). As isotype control nonspecific FITC (Becton Dickinson, Franklin Lakes, New Jersey, USA, #550616), PE (Becton Dickinson, Franklin Lakes, New Jersey, USA, #562141) and PE-Cy5 (Becton Dickinson, Franklin Lakes, New Jersey, USA, #550618) coupled antibodies were used. After incubation for 30 minutes at 4 C°, the cells were washed with PBS and resuspended in 500µl PBS for analysis. Cell fluorescence was evaluated by flow cytometry in a FACS Canto (Becton Dickinson, Franklin Lakes, New Jersey, USA) and data were analyzed by using FlowJo software.

Cell cycle analysis. Stable transduced rASC were harvested after selection and seeded with 500.000 cells/T-175 flask in complete medium. After 48 hours of proliferation, the cells were washed twice with PBS and incubated in medium without FCS for additional 48 hours to obtain cells synchronized in G0/G1. By re-adding FCS containing medium, the cells start to enter the cell cycle and samples are taken 72 hours after FCS addition. Cell pellets were washed with cold PBS/2%BSA and fixed with a methanol-acetone mixture. Staining of DNA content with propidium-iodide (50µg/ml for $1x10^6$ cells in 500µl) was performed after RNase (1mg/ml) (both Sigma, St. Louis, Missouri, USA) treatment for 1hour at 37°C. Nuclei were analyzed in FACS Canto (Becton Dickinson, Franklin Lakes, New Jersey, USA).

Osteogenic and adipogenic differentiation

Osteogenic differentiation was induced when rBMSC and rASC reached 90-100% confluency. High glucose medium (4.5 g/L glucose) (Life Technologies, Carlsbad, California, USA) was supplemented with 10% FCS, 1% P/S, 100nM Dexamethasone, 50µg/ml L-ascorbic acid-2-phosphate and 10 mM ß-glycerol phosphate (all Sigma, St. Louis, Missouri, USA) for 3 weeks. To control osteogenic differentiation, calcium precipitates were analysed with Alizarin RedS (Sigma, St. Louis, Missouri, USA) histochemical staining.

Adipogenic differentiation was induced in 80% confluent rASC and rBMSC cultures by supplementing the cell culture medium with 10µg/ml Insulin, 1µM Dexamethasone and 0,5mM 3-Isobutyl-1-methylxanthin (IBMX) (all Sigma, St. Louis, Missouri, USA) for up to 21 days. After 21 days, histochemical staining with Oil Red O (Sigma, St. Louis, Missouri, USA) was performed to detect lipid droplet formation.

Preparation of plasmids and retroviral transduction

A retroviral transduction system was established for generating a stable *Sox9* gene knockdown in rASC.

Sox9-shRNA sequences were selected using algorithm promoted by Clontech (BD Bioscience, San Jose, California, USA), manufactured at MWG (Ebersberg, Germany), ligated into a shRNA expression vector (RNAi-ready pSIREN retro Q plasmid expression vector) and transfected in a packaging cell line (EcoPack™2-293) (Clontech, BD, Bioscience, San Jose, California, USA). The control expression vector contains a scrambled (no specific target) shRNA sequence.

Replication-incompetent retroviral particles, produced by the packaging cell line (EcoPack™2-293) were used to transduce rASC.

Therefore, cells were seeded in P2 at a low density. After 24 hours of proliferation, the transduction was performed on three consecutive days by adding medium supernatant of the virus producing cells containing fresh virus and culture medium containing 6µg/ml polybren (Sigma, St. Louis, Missouri, USA) at the ratio of 1:1 to the rASC. As controls for the Sox9 knockdown experiments, a scrambled shRNA containing virus was used. Subsequently, transduced rASCs were subjected to selection with puromycin (Sigma, St. Louis, Missouri, USA) to generate a stable vector integration and knockdown of Sox9. Sox9 knockdown cells showing more than 50% reduction of Sox9 gene and protein expression were used for further analysis.

Growth kinetics

To determine the duplication rate of proliferating rASC, the cells were seeded in a low density and cell number was determined every 24 hours using a Cedex counter (Roche, Penzberg, Germany). Doubling time calculation:

$T_d = T \times \log(2) / \log(Nt/N0)$

T_d= doubling time, T: time when cell numbers increased from N0 to Nt; N0: initial cell numbers; Nt: final cell numbers after culture time.

BrdU incorporation assay

Cell proliferation was quantified with a BrdU – ELISA based assay (Roche, Penzberg, Germany) according to manufacturer's protocol.

Transduced and selected cells were seeded in 96-well plates. After 24 hours, culture medium was changed to medium containing BrdU. After additional 24 hours, the amount of BrdU incorporated into the cells was determined by chemiluminescence (binding of a mouse anti-BrdU antibody conjugated with horseradish peroxidase). After colour development the signal was monitored at 450/690 nm in an ELISA reader (Tecan, Männedorf, Swiss).

Table 1. Primer sequences for real-time PCR

Gene name	Primer-Sequenz (5'→3')	Amplicon-length [bp]	Tm [°C]	Acc.No.
Alp (alkaline phosphatase)	fwd: GACAAGAAGCCCTTCACAGC rev: ACTGGGCCTGGTAGTTGTTG	118	59,4 59,4	NM_013059.1
ß-act (Beta actin)	fwd: GTA GCC ATC CAG GCT GTG TT rev: CCC TCA TAG ATG GGC ACA GT	104	60 59	NM_031144
Bcl-2	fwd: GGGAGCGTCAACAGGGAGATG rev: GACAGCCAGGAGAAATCAAACAGAG	169	63,7 63	NM_016993.1
Runx2	fwd: GGCCGGGAATGATGAGAACTA rev: AGATCGTTGAACCTGGCCACT	233	60 60	XM_346016
Ccnd1(Cyclin D1)	fwd: GGAGTGTGGTGGCCGCGATG rev: ACGTCGGTGGGTGTGCAAGC	253	65,5 63,5	NM_171992.4
Col1a1 (collagen1a1)	fwd: TCCAGGGCTCCAACGAGA rev: GCTGTAGGTGAATCGACTGTTGC	59	59 60	Z78279
Dlx3	fwd: CGTTTCCAGAAAGCCCAGTA rev: CCCGGGAGGGGGTCACTCTC	173	65,5 67,6	XM_575377.4
Dlx5	fwd: CTGGCCGCTTTACAGAGAAG rev: CTGGTGACTGTGGCGAGTTA	220	59,4 59,4	NM_012943.1
Itga11 (Integrin alpha 11)	fwd: AACTTCCAGCTCCTGGACAC rev: CTCAGCACCTGTTGGCAGTA	236	59.4 59,4	NM_001108156.1
Mmp13	fwd: ACCTGGGATTTCCAAAAGAGG rev: ACACGTGGTTCCCTGAGAAGA	93	58 58	NM_133530.1
Msx2	fwd: CCTCGGTCAAGTCGGAAAAT rev: ACTGTTTCTGGCGGAACTTG	192	57,3 57,3	NM_012982.3
Bglap (osteocalcin)	fwd: CATGAGGACCCTCTCTCTGC rev: TGGACATGAAGGCTTTGTCA	190	58,4 58,6	NM_013414.1
p21	fwd: AGCAAAGTATGCCGTCGTCT rev: ACACGCTCCCAGACGTAGTT	161	57,3 59,4	BC100620
Sox5	fwd: GAGCAGATCGCAAGGCA rev: CGGGAGGGAACACGGGAATC	120	61,8 63,5	XM_342784.3
Sox6	fwd: GAAATCCATGTCCAACCAGGAG rev: CGGGCCTGCTCTTCATAGTAAG	51	59 59	XM_215016
Sox9	fwd: CTG AAG GGC TAC GAC TGG AC rev: TAC TGG TCT GCC AGC TTC CT	140	59 60	XM_343981
Vegfα	fwd: TGGCTTTACTGCTGTACCTCCA rev: TTTCTGCTCCCCTTCTGTCGT	71	59 60	NM_031836
p300	fwd: ACGCATTGTCCATGACTACAAG rev: CCTCTCTTCCTCTTCTGTTCA	151	58,4 60,3	XM_576312.4

Caspase-3/7 assay

By using the Apo-ONE Homogeneous Caspase-3/7 assay (Promega, Fitchburg, Wisconsin, USA) we measured the caspase-3/7 enzymatic activity as indicator of apoptosis according to manufacturer's instructions. A non-fluorescent caspase substrate (Z-DEVD-R110), added to the ASC, was cleaved into fluorescent molecules with an emission maximum at 521nm in an ELISA reader (Tecan, Männedorf, Swiss).

Protein extraction and Westernblot analysis

rASC were washed with PBS, detached with Trypsin-EDTA, harvested and lysed. Cell lysates were prepared with RIPA Buffer (Thermo Scientific, Waltham, Massachusetts, USA) containing phosphatase and proteinase inhibitors (Roche, Penzberg, Germany). Protein concentration of cell lysates was quantified with a BCA-Assay (Thermo Scientific, Waltham, Massachusetts, USA) and subsequently 25-50 µg protein (depending on the protein of interest) was boiled for 5 min with SDS-sample buffer containing ß-mercaptoethanol and subjected to 10%-12% SDS-PAGE. After electrophoretic separation, the proteins were transferred to nitrocellulose membranes (Bio-Rad, Hercules, California, USA) or PVDF membranes (Roche, Penzberg, Germany). Blotted membranes were blocked with either 5% dry milk or 5% BSA and subsequently incubated with the following primary antibody for 16 hours at 4°C or 1 hour at RT: rabbit polyclonal anti-Sox9 (Millipore, Billerica, Massachusetts, USA, #AB5535), mouse monoclonal anti-p21 (BD Bioscience, San Jose, California, USA, #556430), mouse monoclonal anti-Cyclin D1 (BD Bioscience, San Jose, California, USA, #554180). Equal loading was verified with rabbit monoclonal antibody to ß-actin (Abcam, Cambridge, UK, #AB8227). After washing, the membranes were incubated with the appropriate horseradish peroxidise coupled secondary antibody (Santa Cruz Biotechnology, Santa Cruz, California, USA, and Jackson Immuno Research, West Grove, Pennsylvania, USA). Proteins were detected using ECL detection reagents (Thermo Scientific, Waltham, Massachusetts, USA).

Osteocalcin EIA

Quantification of osteocalcin in 50µg total cell lysates (RIPA) was performed according to the manufacturer's instruction using the Rat Osteocalcin High Sensitive EIA Kits (TAKARA, Shiga, Japan). The samples were read at 450 nm in duplicate using a microplate reader (Tecan, Männedorf, Switzerland).

RNA isolation and real time RT-PCR

Total RNA was isolated using Stratagene's Absolutly RNA Miniprep Kit (Stratagene, La Jolla, California, USA) according to the manufacturer's instructions. To generate single-stranded cDNA, RNA was reverse transcribed with AffinityScript QPCR cDNA Synthesis Kit (Agilent Technologies, Santa Clara, California, USA). PCR was performed with the Mx3005P QPCR System from Agilent Technologies (Santa Clara, California, USA) using Brilliant II SYBER Green qPCR Mastermix (Agilent Technologies, Santa Clara, California, USA). The cDNA copy number of *Sox9* in total RNA was measured using a standard curve generated with serially diluted plasmids containing the PCR amplicon sequences (range of cDNA copy number: 50-500.000 copies). All other genes were analyzed according to the relative quantification method and normalized to ß-actin using primers which are listed in Table 1.

Densitometric quantification of Alizarin Red S staining

Darkly stained area (dark red and black) were analysed densitometrically using Photoshop CS3. Thereby, the pixel number of stained area were measured and related to the total area.

Statistical Analysis

Statistical analyses were performed using GraphPad Prism 4. Two-tailed Mann-Whitney-U test was used, determining if the medians of two groups are significant different. Exact p-values were calculated.

Results

Immunophenotype and differentiation potential of rASC versus rBMSC

We isolated mesenchymal stem cells from the subcutaneous adipose tissue (ASC) and from the bone marrow (BMSC) of five week old CD-rats, and cultured the cells up to passage 2. Application of osteogenic and adipogenic differentiation conditions, using specific culture medium supplements, confirmed differentiation potential which was documented via histological staining (Fig. 1A). The immunophenotypic profile showed that both cell types, rASC as well as rBMSC, are more than 96% CD90 positive in passage 1 and 2, and nearly completely negative for CD45 and CD11b. In contrast to rASC however, rBMSC in passage 1 included 11% CD11b positive cells (leukocyte marker), which decreased in passage two to 1% (Fig. 1B).

Gene expression profile of rASC in comparison to rBMSC

To compare the gene profile of rASC and rBMSC during the first two passages, we quantified the expression of a set of marker genes in passage 1 and 2 including *alkaline phosphatase (Alp), Col1a1, osteocalcin (Bglap), Mmp13, Runx2, Sox9, Vegfα* and *Integrin α11(Itga 11)*, which are known to be important in stem cell biology and differentiation.

In passage 1 (P1), rASC displayed a 4-fold higher gene expression of *Vegfα* as rBMSC. In contrast, *Alp, Mmp13, Itga11* and *osteocalcin* gene expression was profoundly reduced in rASC compared to rBMSC. The gene expression level of *Col1a1, Sox9 and Runx2* was not significantly different in rASC compared to rBMSC (Fig. 2A).

In passage 2 (P2), especially the expression of the transcription factor *Sox9* was strikingly upregulated. *Sox9* was more than 10^3-fold higher expressed in rASC compared to rBMSC. Also *Runx2*, *Vegf*α, *osteocalcin, Itga11* and *Col1a1* gene expression was clearly induced in rASC while *Mmp13* gene expression was downregulated and *Alp* was comparable to rBMSC (Fig. 2B).

As the *Sox9* RNA level was highly induced in rASC compared to rBMSC, we determined Sox9 protein amount. Western blot analysis showed an increase of the Sox9 signal from P1

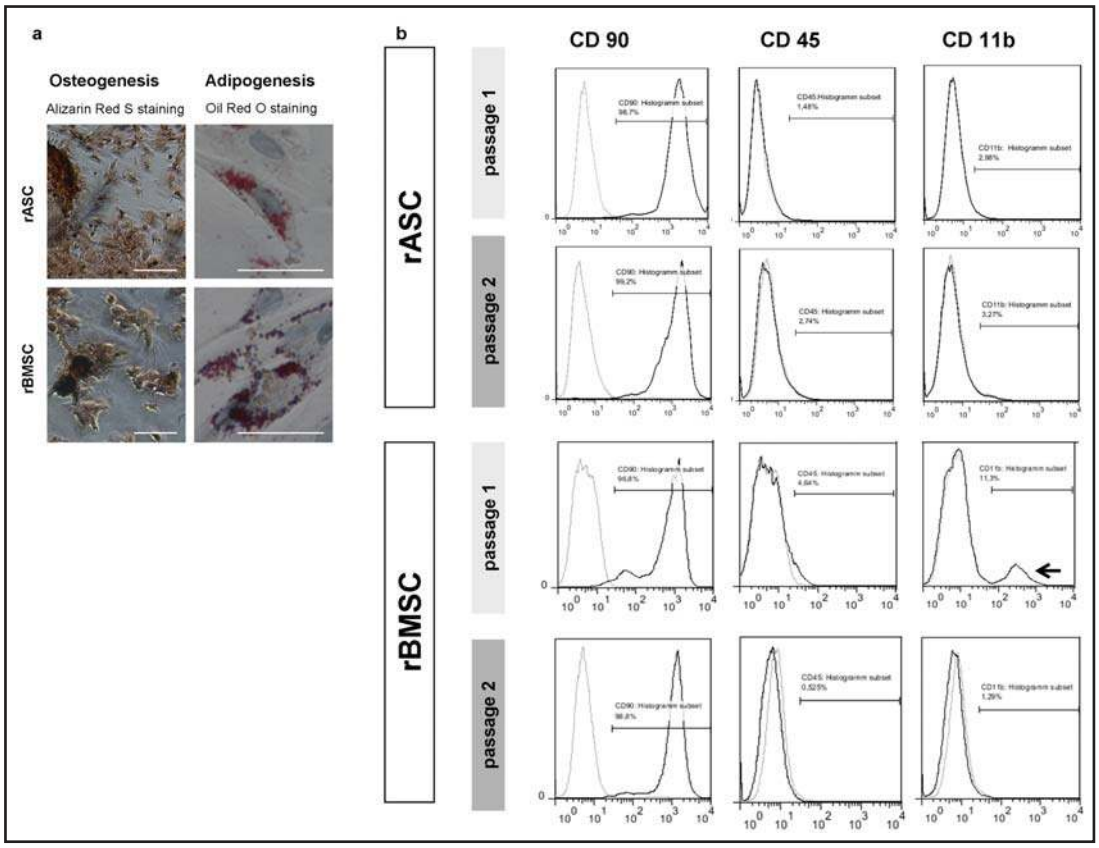

Fig. 1. Characterization of osteo- and adipogenic differentiation and immunophenotype of rASC and rBMSC. a) Mineralization after osteogenic induction was visualized using Alizarin Red S staining, and lipid droplets in adipogenic differentiated MSC were stained with Oil Red O solution. Scale bar = 100µm. b) Flow cytometric analysis of MSC with specific antibodies against CD90, CD45 and CD11b (black line). Arrow indicates CD11b positive cells. Gray line shows isotype controls. Horizontal lines indicate cut-off for positive reactivity. X-axes = intensity log values, y-axes = cell counts.

to P2 in rASC, whereas in rBMSC the signal strength remained approximately the same (Fig. 2C). Comparison of *Sox9* gene expression, calibrated on rASC P1, revealed a strong increase between P1 and P2 in rASC while in rBMSC *Sox9* mRNA expression was reduced (Fig. 2D).

Retroviral-mediated Sox9 knockdown in rASC affected proliferation, p21 and Cyclin D1 protein expression and gene expression of osteogenic markers

As we observed a significantly higher mRNA and protein expression of Sox9 in rASC compared to rBMSC in passage 2 (Fig. 2B, C, D), we addressed the role of this transcription factor in undifferentiated rASC with respect to cell growth and differentiation. Possibly, increased Sox9 expression is a major distinguishing feature between ASC and BMSC and might explain differences in the biology of these two adult stem cell types.

For a more detailed functional analysis of the transcription factor, we next stably silenced Sox9 in rASC. Sox9 mRNA and protein level were significantly reduced via shRNA. *Sox9* cDNA copies (per 100ng RNA) declined from about 12.000 to 4000 on average which is ~ 70% reduction of expression (Fig. 3A), and accordingly the protein signal was strongly reduced in western blots (Fig. 3B). In the following, Sox9 knockdown cells are termed "–SOX9" and all knockdown experiments were carried out with passage 2 rASC.

One well known difference between ASC and BMSC is the higher proliferation rate of ASC. Therefore, we analysed the proliferative activity after Sox9 silencing in rASC. Growth kinetics demonstrated that after 72 hours of proliferation, the number of control cells

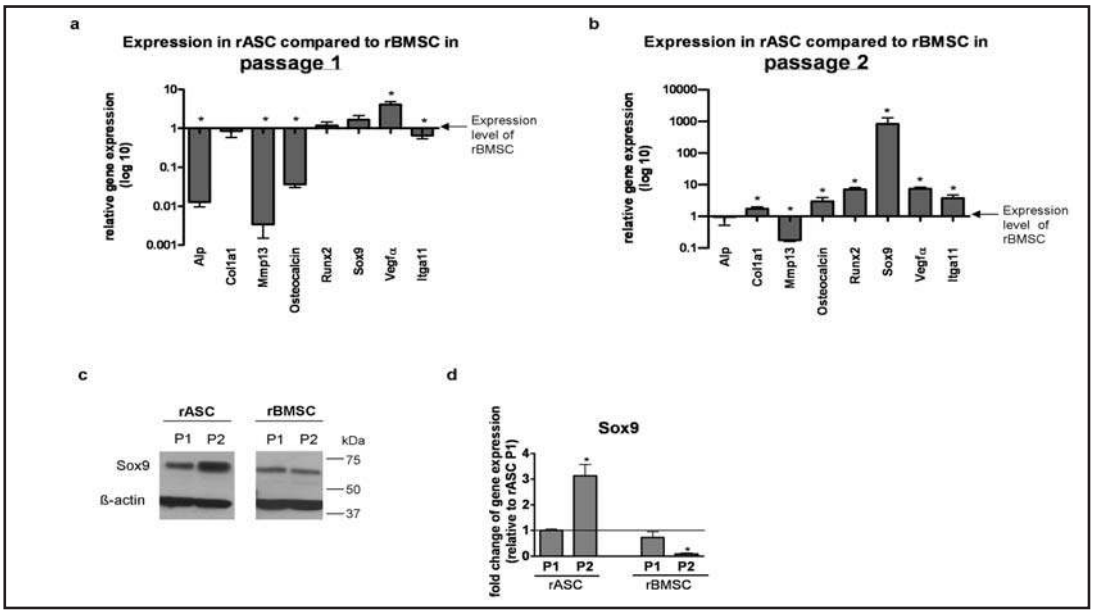

Fig. 2. Gene expression profile of rASC versus rBMSC. Relative gene expression quantification of rASC and rBMSC in passage 1 (a) and passage 2 (b). Gene expression of rBMSC was set as calibrator and constitutes the x-axis at 1. Results are mean +/- SEM. n= 4; * p< 0,05. c) Representative western blotting image demonstrates protein expression of Sox9 in rASC and rBMSC in P1 and P2. Cells were lysed in RIPA buffer and separated by SDS-PAGE. After immunoblotting, Sox9 was detected with an anti-Sox9 antibody and equal loading was controlled by an anti-ß-actin antibody. n= 3. d) *Sox9* gene expression for rASC and rBMSC in P1 and P2. Results are calibrated on rASC of P1, normalized to housekeeping gene β-actin, and show mean +/- SEM. n= 4; * p< 0,05.

Fig. 3. Silencing of Sox9 in rASC. Sox9 mRNA and protein expression after Sox9 knockdown was compared to mock-transfected control rASC. a) Quantitative PCR revealed a 70% decrease of *Sox9* cDNA copies in retroviral transduced rASC. b) Western Blot analysis showed a strongly decreased Sox9 protein signal compared to control cells. Results are mean +/- SEM. * p< 0,05. n=6

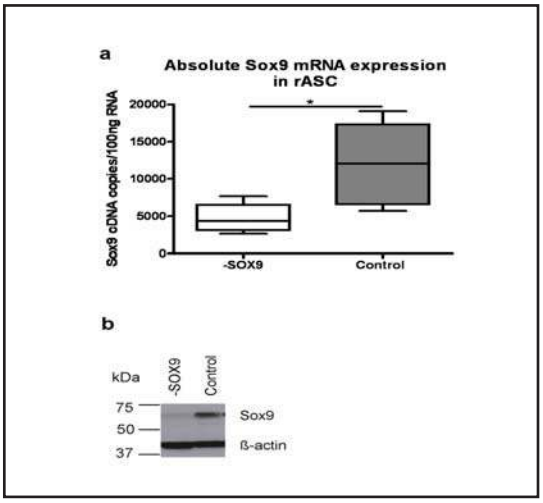

(transfected with a scrambled shRNA construct = mock transfected) was significant higher compared to –SOX9 cells (Fig. 4A). From that data, we calculated a doubling time of –SOX9 rASC of about 60,96 hours days while control cells needed about 52,56 hours.

BrdU incorporation assay displayed a 20% decreased BrdU signal in –SOX9 cells (Fig. 4B) and cell cycle analysis using flow cytometry demonstrated a significant decrease of S-phase cells in the –SOX9 rASC population compared to control cells (Fig. 4C).

Next we determined gene and protein expression of the cell cycle inhibitor p21 in –SOX9 rASC and controls. The p21 protein signal was strongly increased in –SOX9 cells compared to control cells (Fig. 4D). However, the mRNA level of *p21* was not affected after Sox9 silencing (Fig. 4E).

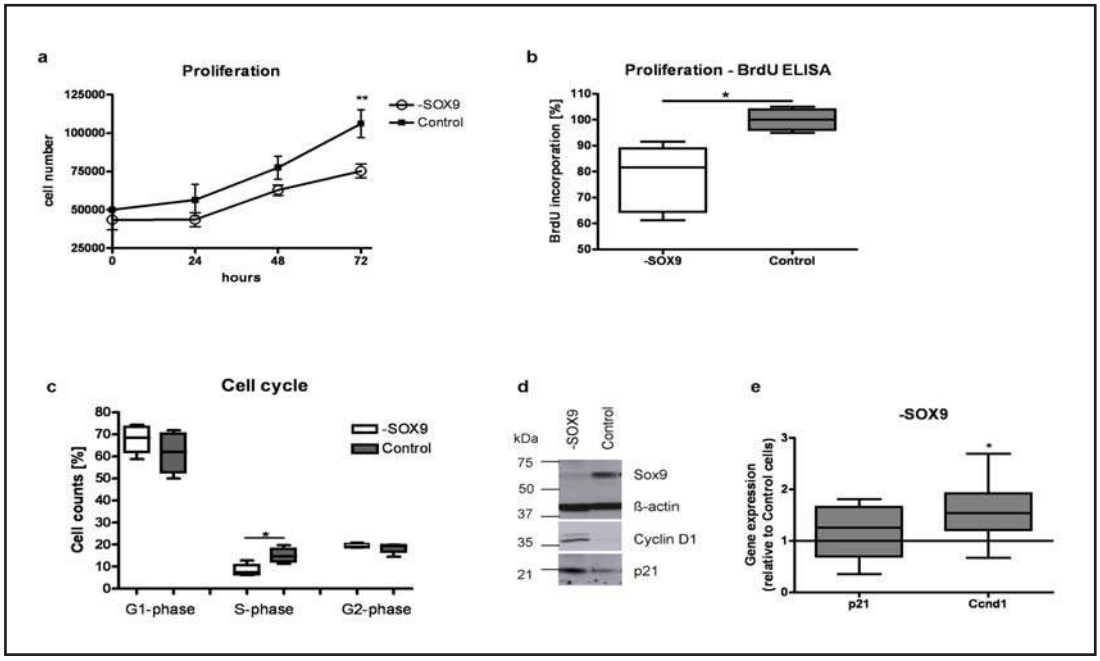

Fig. 4. Proliferation and apoptosis in -SOX9 rASC. a) Growth kinetics displayed a highly significant diminished proliferation rate in –SOX9 rASC after 72 hours. b) BrdU incorporation assay revealed a 20% reduced BrdU labelling of –SOX9 rASC. c) Cell cycle analysis via FACS revealed a diminished –SOX9 rASC S-phase population. d) Westernblot evaluation showed increased p21 and cyclin D1 protein signals in –SOX9 rASC. e) Cyclin D1 gene expression was significantly up regulated while p21 mRNA level was not affected. Results are mean +/- SEM. * p<0,05; ** p < 0,01. n = 4.

Fig. 5. Analysis of apoptotic activity in -SOX9 rASC. a) Caspase 3/7 activity assay demonstrated no changes in apoptotic activity of –SOX9 rASC versus controls. b) Expression of anti-apoptotic gene *Bcl-2* was not regulated in –SOX9 rASC compared to control. Results are mean +/- SEM. n=3.

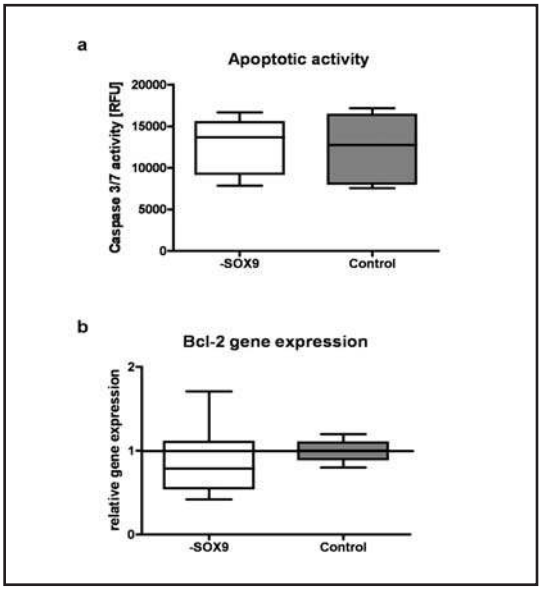

In addition, we analysed the protein and mRNA expression of cyclin D1, a cell cycle activator, after Sox9 knockdown. We observed an increase in cyclin D1 protein signal (Fig. 4D) and a significant higher gene expression of *Ccnd1* (cyclin D1) in –SOX9 rASC compared to controls (Fig. 4E).

To ensure that the decrease of proliferation (Fig. 4A) and the diminished BrdU signal (Fig. 4B) is not due to decreased cell viability in the –SOX9 rASC population, we determined

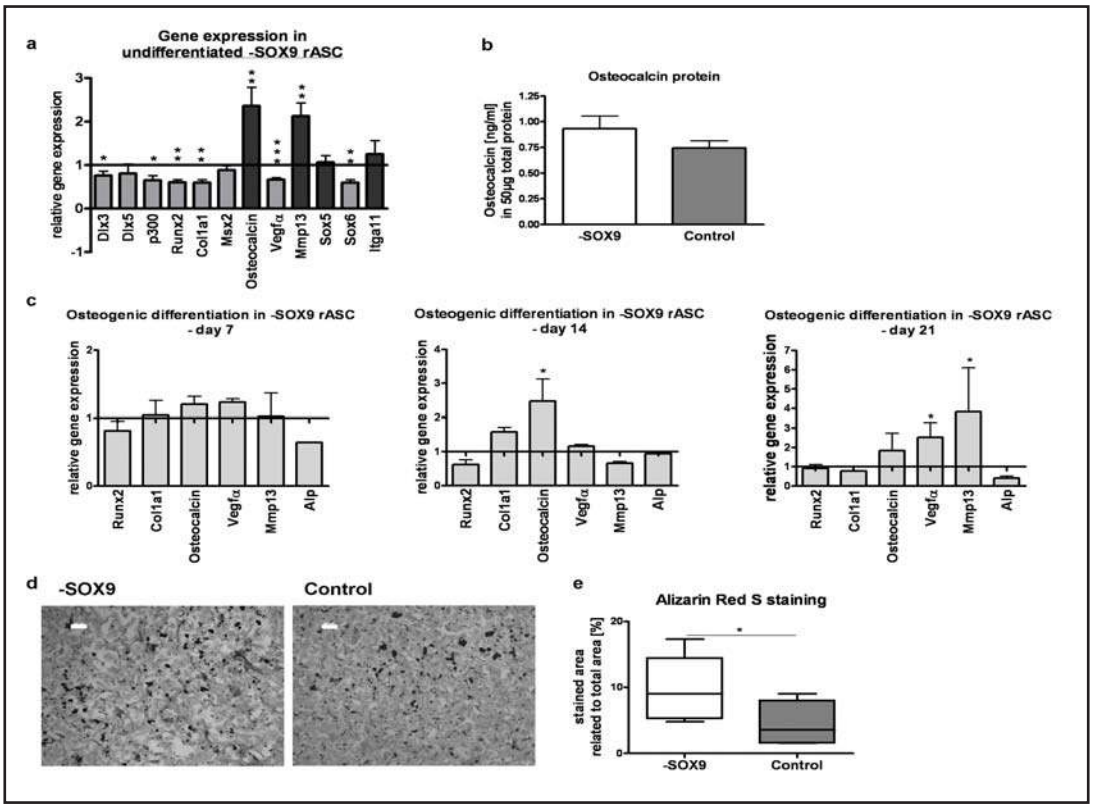

Fig. 6. Expression of osteogenic markers and staining of mineralization nodules in –SOX9 rASC. a) Relative gene expression analysis after Sox9 knockdown in undifferentiated rASC. Results are mean +/- SEM. * p<0,05; ** p<0,01; *** p<0,001; n=7-9. b) Osteocalcin protein concentration in undifferentiated –SOX9 and control rASC cell lysates [ng/ml] per 50µg total protein; n=4. c) Expression of osteogenic markers after 7,14 and 21 days of osteogenic differentiation in –SOX9 rASC which were calibrated on control cells and normalized to housekeeping gene. Results are mean +/- SEM. * p<0,05; n=4. d) Alizarin Red S staining of –Sox9 rASC and control rASC after 21 days of osteogenic differentiation; Scale bar = 200µm; n=5. e) Densitometric measurement of Alizarin Red S stained areas by calculating the pixel number of stained nodules in relation to the pixel number of the total area. Results are mean +/- SEM. * p<0,05; n=5.

the apoptotic activity via a caspase 3/7 activity assay (Fig. 5A) and the expression of the anti-apoptotic gene *Bcl-2* (Fig. 5B). We found no evidence for changes in caspase 3/7 activity and *Bcl-2* mRNA level after Sox9 silencing and thus excluded alteration in apoptosis rate as a consequence of reduced proliferation.

Induction of osteocalcin and Mmp13 expression after Sox9 inhibition in undifferentiated rASC

As Sox9 downregulation is a prerequisite for osteogenic differentiation of progenitor cells during embryonic musculoskeletal development, we analysed the expression profile of marker genes related to osteogenic differentiation in undifferentiated –SOX9 rASC.

Among the thirteen analysed genes, only *osteocalcin* and *Mmp13* mRNA levels were significantly up regulated in undifferentiated rASC after Sox9 knockdown (Fig. 6A). Analysis of protein expression showed an increase of osteocalcin concentration in –SOX9 cell lysates by trend (Fig. 6B). For –SOX9 rASC, the osteocalcin concentration varied between 1,3 – 0,7 ng/ml and for control cells between 0,9 and 0,5 ng/ml per 50µg total protein. *Dlx3, p300, Runx2, Col1a1, Vegfα* and *Sox6* gene expression level were decreased in –SOX9 rASC compared to controls, whereas mRNA level of *Dlx5*, *Msx2*, *Sox5* and *Itga11* were not affected.

Increased gene expression of osteocalcin, Mmp13 and Vegfα during osteogenic differentiation in –SOX9 rASC

Here, we analysed whether the progression of *in vitro* osteogenic differentiation is affected by the Sox9 dose in rASC.

In undifferentiated –SOX9 rASC markers for late osteogenesis like *osteocalcin* and *Mmp13* were induced, and the expression of early markers like *Runx2, Col1a1* and *Vegfα* were downregulated (Fig. 6A), however after 7 days of osteogenic differentiated, none of these genes was regulated at this time point (Fig. 6C).

Gene expression analysis after 14 days of osteogenic differentiation demonstrated that *osteocalcin* gene expression is significantly increased in –SOX9 cells, whereas *Mmp13* and *Alp, Vegfα, Runx2* and *Col1a1* were not regulated at that time point. However, after 21 days of osteogenesis, *Vegfα* and *Mmp13* mRNA levels were significantly increased and *osteocalcin* by trend (Fig. 6C).

Alizarin Red S staining of the mineralized matrix at the end point at day 21 visualizes an increase in nodule formation for –SOX9 rASC compared to controls (Fig. 6D), which was quantified densitometrically by calculating the pixel number of the stained area in relation to the total area (Fig. 6E). For –SOX9 cells at average 9% of the total area was stained with Alizarin Red S, whereas control cells display only 4% staining at average.

Discussion

In order to promote usage of ASC in the field of regenerative medicine, it is crucial to compare them with the better characterized BMSC with respect to cell activity and differentiation potential. Here, we analyzed the gene expression profile of some differentiation and stem cell biology markers between undifferentiated rASC and rBMSC in passage 1 and 2 which revealed significant discrepancies.

The α11*ß*1 integrin receptor plays a major role in mediating the crosstalk and cell adhesion between MSC and the surrounding ECM via collagen I binding [32]. Therefore, the higher *Integrin α11* expression in rASC compared to rBMSC might indicate an advantage in cellular processes, such as cell adhesion, migration and differentiation in general between the two cell types. Being moreover a marker for differentiation in MSC, a high Integrin α11 level is associated with less differentiation pointing to a higher "stemness" of ASC even in later passages [33].

Among others, Runx2 is a crucial transcription factor that regulates bone formation during early embryogenesis. Our results indicated increased *Runx2* expression in rASC versus rBMSC in passage 2 together with a profoundly induced *Sox9* expression. Runx2 is a key regulator of osteoblast-specific gene expression. Various studies have verified that induction of Runx2 commits MSC to osteogenesis through mediating expression of other osteogenic-target genes, such as *Col1a1*, and *osteocalcin* [34, 35]. In addition, Runx2 can also serve as a transcription factor to induce transcription of *Vegfα* which is regulated via Runx2 in a tissue specific manner during endochondral bone formation [36]. Surprisingly, we noticed increasing *osteocalcin* gene expression in undifferentiated rASC in passage 2 compared to rBMSC. This observation indicates that osteocalcin might not be as specific for osteoblasts as postulated by Ducy et al., who suggests that osteocalcin protein is specifically synthesized by osteoblasts and is a marker of osteoblast differentiation during the later stages of bone formation [37]. We unambiguously detected osteocalcin protein in cell lysates of undifferentiated rASC indicating extra functions of osteocalcin besides Ca^2-binding which might be related to insulin metabolism. Ex vivo, picomolar amounts of osteocalcin can stimulate cyclin D1 and insulin gene expression plus proliferation markers in beta-cells whereas nanomolar amounts induce adiponectin expression, an insulin-sensitizing adipokine, in adipocytes. Thus osteocalcin evolved as a novel molecular player which augments the effects of insulin and that way regulates glucose metabolisms and fat mass in the body [38, 39].

The most striking increase in gene and protein expression was found for transcription factor Sox9. Being on approximately the same level in rASC and rBMSC in P1, the mRNA level was up to 10^3-fold higher in rASC in comparison to rBMSC in P2 and moreover the protein level was clearly increased. That points to a crucial role for Sox9 in ASC which appears not to be restricted to differentiation processes per se.

To elucidate putative functions of Sox9 in undifferentiated rASC, we silenced Sox9 via retroviral transduction and analysed the downstream effects. We observed a clear decrease in proliferative activity of rASC without increase in apoptotic activity. Concomitantly, we detected an increased protein level of the cell cycle inhibitor *p21*, however without an increase in gene expression what points to a post-transcriptional regulation of p21 mRNA as it was already shown for 3T3-L1 pre-adipocytes [40]. We suggest that in native ASC, the p21 protein signal decreases over passages which might be related to the higher Sox9 expression in rASC compared to rBMSC, as a Sox9 knockdown dramatically increases p21 protein expression indicating a pro-proliferative role of Sox9. This is in line with a recent report which described that the p21 expression is decreased in ASC compared to BMSC in patients with osteoporotic fractures, suggesting that this may be one reason for the higher proliferation potential of ASC. The authors concluded that proliferation and osteogenic differentiation of ASC were less affected by age and multiple passaging than BMSC, suggesting that ASC have the potential to become a more effective therapeutic option for cell-based therapy, especially in elderly patients with osteoporosis [41].

In this line, –SOX9 rASC displayed a significant decrease of S-phase cells compared to control cells. It is known that p21 functions as a regulator of cell cycle progression of the G1/S-phase transition [42], leading to the conclusion that the high p21 level in Sox9 knockdown cells impairs the S-phase entry. On the basis of observations from Peng et al. [43] and other groups that observed a higher proliferation rate in ASC vs. BMSC, we suppose that at least in part, the profoundly higher Sox9 level in ASC contributes to the higher proliferation rate.

As it is known that the cell cycle inhibitor p21 is closely related to cyclin D1, we also analysed cyclin D1 level in undifferentiated rASC. We observed an increase in cyclin D1 protein together with the mRNA level as a consequence of Sox9 inhibition. That may suggest precocious senescence of the cells, according to Alt et al., who postulated that the accumulation of cyclin D1 in senescent cells may be due to elevated level of p21 [44] . Consequently, Sox9 is not only pro-proliferative, but also might prevent the cells from undergoing early senescence, what again supports the importance of proper Sox9 expression in undifferentiated stem cells. Coleman and co-workers proposed that an increase in cyclin D1 is sufficient to inhibit the proteasome-mediated degradation of p21 [45], hence a strongly elevated cyclin D1 level might potentiate delay in cell cycle progression by stabilizing p21 protein.

Besides being crucial for the cell cycle distribution, cyclin D1, a target of ß-catenin, is known to be required for the propagation of specific types of osteoprogenitor cells at various developmental stages during calvarial morphogenesis. Mirando et al. showed several calvarial abnormalities of cyclin D1 -/- mice, like a delayed ossification at the newborn stage, decreased mineralization and a wider suture region and suggest as underlying mechanism an impairment of osteoblast development caused by the loss of cyclin D1 [46]. This is interesting in the context of our observation that the expression profile of undifferentiated and osteogenic induced rASC after Sox9 inhibition revealed an induction of *osteocalcin* and *Mmp13* suggesting a pro-osteogenic effect after Sox9 inhibition which in part might be mediated through cyclin D1.

Notably, *Vegfα, Sox6, Col1a1, Dlx3, p300* and *Runx2* were down regulated in undifferentiated -SOX9 cells indicating a decrease in the general differentiation capacity of MSC. Most likely, the impact of the transcription factor Sox9 is strictly differentiation stage and dose specific, like it was shown for pre-hypertrophic chondrocytes where Sox9 prevented osteoblastic differentiation while early in development Sox9 is required to maintain growth plate chondrocyte proliferation [47]. Notably, the proliferation rate of expanded MSC showed a positive correlation with chondrogenesis suggesting that growth and differentiation steps are closely coordinated and resemble stages known from embryonic cartilage development

[48]. Possibly, too early inhibition of Sox9 expression in still undifferentiated MSC in general impairs proliferation and in consequence also differentiation capacity of the cells.

The clear upregulation of *osteocalcin* and *Mmp13* in undifferentiated –SOX9 rASC was accompanied by a decrease of *Runx2* and its co-factors *p300, Dlx3* and *Vegfα*. As all of these genes are associated to osteogenic differentiation, we have exposed –SOX9 rASC to *in vitro* osteogenesis for up to 21 days. There are conflicting reports concerning osteogenic capacity of ASC. Hayashi et al. was unable to detect matrix formation or *osteocalcin* expression in rASC [49] whereas other groups described and characterized the osteogenic differentiation potential of ASC in detail [50, 51]. We clearly observed calcium matrix deposits and measured *osteocalcin* mRNA and osteocalcin protein expression under osteogenic favourable culture conditions. During the early phase of osteogenic differentiation, none of the analysed osteogenic marker were regulated in –SOX9 cells, however, on day 14 and day 21, gene expression of *osteocalcin*, *Vegfα* and *Mmp13* was induced. Accordingly, we conclude that Sox9 has no impact on early osteogenic differentiation whereas the expression of osteogenic markers in later phases of *in vitro* osteogenesis were induced when Sox9 dose was less than 50% of controls. Moreover, after 21 days calcium mineralization deposits, as an indicator of successful osteogenesis, are significantly enhanced in –SOX9 rASC compared to control cells.

Venkatesan and co-workers observed a reduced level of Mmp13 when they overexpressed Sox9 in human MSC and differentiated them into chondrocytes [52], and Liang et al. reported that transgenic mice with osteoblast-specific Sox9 expression (Col1a1-Sox9 transgenic) have a significantly lower osteocalcin expression [53]. Accordingly, we suggest an inhibitory effect of Sox9 on *osteocalcin* and *Mmp13* gene expression, as both are upregulated after Sox9 knockdown in undifferentiated and osteogenic differentiated rASC.

Conclusion

In conclusion, our study suggest that Sox9 has a pro-proliferative effect in undifferentiated rASC, presumably via regulation of p21 and cyclin D. Notably, apoptosis rate and apoptosis related gene expression appears not to be affected by Sox9. Reducing the Sox9 dose < 50% of controls impairs proliferation and increases the expression of differentiation related markers as osteocalcin and Mmp13 in undifferentiated and osteogenic differentiated rASC, suggesting the existence of regulatory mechanism of Sox9 with respect to these genes. We suggest that cyclin D1 might be a candidate for mediating the anti-proliferative and pro-osteogenic effects in our rASC study when the Sox9 level is critically reduced.

Acknowledgements

We want to thank Mandy Vogel for her superb technical assistance. This work was supported by the DFG grants GR1301/7-1 and 7-2 assigned to SG.

References

1 Jones EA, Kinsey SE, English A, Jones RA, Straszynski L, Meredith DM, Markham AF, Jack A, Emery P, McGonagle D: Isolation and characterization of bone marrow multipotential mesenchymal progenitor cells. Arthritis Rheum 2002;46:3349-3360.

2 da Silva ML, Chagastelles PC, Nardi NB: Mesenchymal stem cells reside in virtually all post-natal organs and tissues. J Cell Sci 2006;119:2204-2213.

3 Kassis I, Zangi L, Rivkin R, Levdansky L, Samuel S, Marx G, Gorodetsky R: Isolation of mesenchymal stem cells from G-CSF-mobilized human peripheral blood using fibrin microbeads. Bone Marrow Transplant 2006;37:967-976.

4 Zou Z, Zhang Y, Hao L, Wang F, Liu D, Su Y, Sun H: More insight into mesenchymal stem cells and their effects inside the body. Expert Opin Biol Ther 2010;10:215-230.
5 Khan WS, Adesida AB, Hardingham TE: Hypoxic conditions increase hypoxia-inducible transcription factor 2alpha and enhance chondrogenesis in stem cells from the infrapatellar fat pad of osteoarthritis patients. Arthritis Res Ther 2007;9:R55.
6 Fraser JK, Zhu M, Wulur I, Alfonso Z: Adipose-derived stem cells. Methods Mol Biol 2008;449:59-67.
7 Puissant B, Barreau C, Bourin P, Clavel C, Corre J, Bousquet C, Taureau C, Cousin B, Abbal M, Laharrague P, Penicaud L, Casteilla L, Blancher A: Immunomodulatory effect of human adipose tissue-derived adult stem cells: comparison with bone marrow mesenchymal stem cells. Br J Haematol 2005;129:118-129.
8 Frohlich M, Grayson WL, Marolt D, Gimble JM, Kregar-Velikonja N, Vunjak-Novakovic G: Bone grafts engineered from human adipose-derived stem cells in perfusion bioreactor culture. Tissue Eng Part A 2010;16:179-189.
9 Di BC, Farlie P, Penington AJ: Bone regeneration in a rabbit critical-sized skull defect using autologous adipose-derived cells. Tissue Eng Part A 2008;14:483-490.
10 Mitchell JB, McIntosh K, Zvonic S, Garrett S, Floyd ZE, Kloster A, Di HY, Storms RW, Goh B, Kilroy G, Wu X, Gimble JM: Immunophenotype of human adipose-derived cells: temporal changes in stromal-associated and stem cell-associated markers. Stem Cells 2006;24:376-385.
11 Varma MJ, Breuls RG, Schouten TE, Jurgens WJ, Bontkes HJ, Schuurhuis GJ, van Ham SM, van Milligen FJ: Phenotypical and functional characterization of freshly isolated adipose tissue-derived stem cells. Stem Cells Dev 2007;16:91-104.
12 Safwani WK, Makpol S, Sathapan S, Chua KH: Alteration of gene expression levels during osteogenic induction of human adipose derived stem cells in long-term culture. Cell Tissue Bank 2012; Epub ahead of print.
13 Safwani WK, Makpol S, Sathapan S, Chua KH: The impact of long-term in vitro expansion on the senescence-associated markers of human adipose-derived stem cells. Appl Biochem Biotechnol 2012;166:2101-2113.
14 Wuelling M, Vortkamp A: Chondrocyte proliferation and differentiation. Endocr Dev 2011;21:1-11.
15 Akiyama H: Control of chondrogenesis by the transcription factor Sox9. Mod Rheumatol 2008;18:213-219.
16 Akiyama H, Kim JE, Nakashima K, Balmes G, Iwai N, Deng JM, Zhang Z, Martin JF, Behringer RR, Nakamura T, de Crombrugghe B: Osteo-chondroprogenitor cells are derived from Sox9 expressing precursors. Proc Natl Acad Sci U S A 2005;102:14665-14670.
17 Akiyama H, Lefebvre V: Unraveling the transcriptional regulatory machinery in chondrogenesis. J Bone Miner Metab 2011;29:390-395.
18 Lefebvre V, Dumitriu B, Penzo-Mendez A, Han Y, Pallavi B: Control of cell fate and differentiation by Sry-related high-mobility-group box (Sox) transcription factors. Int J Biochem Cell Biol 2007;39:2195-2214.
19 Yang Z, Huang CY, Candiotti KA, Zeng X, Yuan T, Li J, Yu H, Abdi S: Sox-9 facilitates differentiation of adipose tissue-derived stem cells into a chondrocyte-like phenotype in vitro. J Orthop Res 2011;29:1291-1297.
20 Akiyama H, Lyons JP, Mori-Akiyama Y, Yang X, Zhang R, Zhang Z, Deng JM, Taketo MM, Nakamura T, Behringer RR, McCrea PD, de Crombrugghe B: Interactions between Sox9 and beta-catenin control chondrocyte differentiation. Genes Dev 2004;18:1072-1087.
21 Zhou G, Zheng Q, Engin F, Munivez E, Chen Y, Sebald E, Krakow D, Lee B: Dominance of SOX9 function over RUNX2 during skeletogenesis. Proc Natl Acad Sci U S A 2006;103:19004-19009.
22 Hardingham TE, Oldershaw RA, Tew SR: Cartilage, SOX9 and Notch signals in chondrogenesis. J Anat 2006;209:469-480.
23 Goldring MB, Tsuchimochi K, Ijiri K: The control of chondrogenesis. J Cell Biochem 2006;97:33-44.
24 Lee JM, Im GI: SOX trio-co-transduced adipose stem cells in fibrin gel to enhance cartilage repair and delay the progression of osteoarthritis in the rat. Biomaterials 2012;33:2016-2024.
25 Rada T, Reis RL, Gomes ME: Distinct stem cells subpopulations isolated from human adipose tissue exhibit different chondrogenic and osteogenic differentiation potential. Stem Cell Rev 2011;7:64-76.
26 Jiang SS, Fang WT, Hou YH, Huang SF, Yen BL, Chang JL, Li SM, Liu HP, Liu YL, Huang CT, Li YW, Jang TH, Chan SH, Yang SJ, Hsiung CA, Wu CW, Wang LH, Chang IS: Upregulation of SOX9 in lung adenocarcinoma and its involvement in the regulation of cell growth and tumorigenicity. Clin Cancer Res 2010;16:4363-4373.
27 Gartel AL, Serfas MS, Tyner AL: p21--negative regulator of the cell cycle. Proc Soc Exp Biol Med 1996;213:138-149.
28 Griffin SV, Shankland SJ: Not just an inhibitor: a role for p21 beyond the cell cycle-"The truth is rarely pure and never simple". J Am Soc Nephrol 2004;15:825-826.
29 Tholpady SS, Katz AJ, Ogle RC: Mesenchymal stem cells from rat visceral fat exhibit multipotential differentiation in vitro. Anat Rec A Discov Mol Cell Evol Biol 2003;272:398-402.

30 Bunnell BA, Flaat M, Gagliardi C, Patel B, Ripoll C: Adipose-derived stem cells: isolation, expansion and differentiation. Methods 2008;45:115-120.
31 Ahmed N, Vogel B, Rohde E, Strunk D, Grifka J, Schulz MB, Grassel S: CD45-positive cells of haematopoietic origin enhance chondrogenic marker gene expression in rat marrow stromal cells. Int J Mol Med 2006;18:233-240.
32 Barczyk M, Carracedo S, Gullberg D: Integrins. Cell Tissue Res 2010;339:269-280.
33 Halfon S, Abramov N, Grinblat B, Ginis I: Markers distinguishing mesenchymal stem cells from fibroblasts are downregulated with passaging. Stem Cells Dev 2011;20:53-66.
34 Viereck V, Siggelkow H, Tauber S, Raddatz D, Schutze N, Hufner M: Differential regulation of Cbfa1/Runx2 and osteocalcin gene expression by vitamin-D3, dexamethasone, and local growth factors in primary human osteoblasts. J Cell Biochem 2002;86:348-356.
35 Franceschi RT, Xiao G, Jiang D, Gopalakrishnan R, Yang S, Reith E: Multiple signaling pathways converge on the Cbfa1/Runx2 transcription factor to regulate osteoblast differentiation. Connect Tissue Res 2003;44:S109-116.
36 Zelzer E, Glotzer DJ, Hartmann C, Thomas D, Fukai N, Soker S, Olsen BR: Tissue specific regulation of VEGF expression during bone development requires Cbfa1/Runx2. Mech Dev 2001;106:97-106.
37 Ducy P, Desbois C, Boyce B, Pinero G, Story B, Dunstan C, Smith E, Bonadio J, Goldstein S, Gundberg C, Bradley A, Karsenty G: Increased bone formation in osteocalcin-deficient mice. Nature 1996;382:448-452.
38 Ferron M, Hinoi E, Karsenty G, Ducy P: Osteocalcin differentially regulates beta cell and adipocyte gene expression and affects the development of metabolic diseases in wild-type mice. Proc Natl Acad Sci U S A 2008;105:5266-5270.
39 Lee NK, Sowa H, Hinoi E, Ferron M, Ahn JD, Confavreux C, Dacquin R, Mee PJ, McKee MD, Jung DY, Zhang Z, Kim JK, Mauvais-Jarvis F, Ducy P, Karsenty G: Endocrine regulation of energy metabolism by the skeleton. Cell 2007;130:456-469.
40 Fernandes KM, Auld CA, Hopkins RG, Morrison RF: Helenalin-mediated post-transcriptional regulation of p21(Cip1) inhibits 3T3-L1 preadipocyte proliferation. J Cell Biochem 2008;105:913-921.
41 Chen HT, Lee MJ, Chen CH, Chuang SC, Chang LF, Ho ML, Hung SH, Fu YC, Wang YH, Wang HI, Wang GJ, Kang L, Chang JK: Proliferation and differentiation potential of human adipose-derived mesenchymal stem cells isolated from elderly patients with osteoporotic fractures. J Cell Mol Med 2012;16:582-593.
42 Harper JW, Elledge SJ, Keyomarsi K, Dynlacht B, Tsai LH, Zhang P, Dobrowolski S, Bai C, Connell-Crowley L, Swindell E: Inhibition of cyclin-dependent kinases by p21. Mol Biol Cell 1995;6:387-400.
43 Peng L, Jia Z, Yin X, Zhang X, Liu Y, Chen P, Ma K, Zhou C: Comparative analysis of mesenchymal stem cells from bone marrow, cartilage, and adipose tissue. Stem Cells Dev 2008;17:761-773.
44 Alt JR, Gladden AB, Diehl JA: p21(Cip1) Promotes cyclin D1 nuclear accumulation via direct inhibition of nuclear export. J Biol Chem 2002;277:8517-8523.
45 Coleman ML, Marshall CJ, Olson MF: Ras promotes p21(Waf1/Cip1) protein stability via a cyclin D1-imposed block in proteasome-mediated degradation. EMBO J 2003;22:2036-2046.
46 Mirando AJ, Maruyama T, Fu J, Yu HM, Hsu W: beta-catenin/cyclin D1 mediated development of suture mesenchyme in calvarial morphogenesis. BMC Dev Biol 2010;10:116.
47 Dy P, Wang W, Bhattaram P, Wang Q, Wang L, Ballock RT, Lefebvre V: Sox9 directs hypertrophic maturation and blocks osteoblast differentiation of growth plate chondrocytes. Dev Cell 2012;22:597-609.
48 Dexheimer V, Frank S, Richter W: Proliferation as a requirement for in vitro chondrogenesis of human mesenchymal stem cells. Stem Cells Dev 2012;21:2160-2169.
49 Hayashi O, Katsube Y, Hirose M, Ohgushi H, Ito H: Comparison of osteogenic ability of rat mesenchymal stem cells from bone marrow, periosteum, and adipose tissue. Calcif Tissue Int 2008;82:238-247.
50 Arrigoni E, Lopa S, de GL, Stanco D, Brini AT: Isolation, characterization and osteogenic differentiation of adipose-derived stem cells: from small to large animal models. Cell Tissue Res 2009;338:401-411.
51 Choi JW, Park EJ, Shin HS, Shin IS, Ra JC, Koh KS: In Vivo Differentiation of Undifferentiated Human Adipose Tissue-Derived Mesenchymal Stem Cells in Critical-Sized Calvarial Bone Defects. Ann Plast Surg 2012; Epub ahead of print.
52 Venkatesan JK, Ekici M, Madry H, Schmitt G, Kohn D, Cucchiarini M: SOX9 gene transfer via safe, stable, replication-defective recombinant adeno-associated virus vectors as a novel, powerful tool to enhance the chondrogenic potential of human mesenchymal stem cells. Stem Cell Res Ther 2012;3:22.
53 Liang B, Cotter MM, Chen D, Hernandez CJ, Zhou G: Ectopic expression of SOX9 in osteoblasts alters bone mechanical properties. Calcif Tissue Int 2012;90:76-89.